Alignment of He- and H-like P states of 48-MeV foil-excited Mg ions

J. Palinkas* and G. J. Pedrazzini
Cyclotron Institute, Texas A&M University, College Station, Texas 77843

D. A. Church and R. A. Kenefick
Cyclotron Institute and Department of Physics, Texas A&M University, College Station, Texas 77843

C. A. Fulton and R. L. Watson
Cyclotron Institute, Texas A&M University, College Station, Texas 77843

D.-W. Wang†
Cyclotron Institute and Department of Physics, Texas A&M University, College Station, Texas 77843
(Received 20 August 1984)

The angular distributions of the ^1P, ^3P, and ^2P lines of 2-MeV/amu Mg projectiles excited by collision with carbon and aluminum atoms in thin foils have been measured with a pivoted plane-crystal Bragg spectrometer. Both the polarizations of these lines and the reflection properties of the ammonium dihydrogen phosphate (ADP) diffraction crystal have been determined. The σ_0/σ_1 cross-section ratios for populating the $2p(|m|=0)$ and $2p(|m|=1)$ states in the $1s2p$ He-like and the $2p$ H-like configurations were deduced from the polarization values and compared with the coupled-states calculation of Reading *et al.*, assuming that the mechanism populating these states is the capture of electrons from the K shell of the target. The agreement between theory and experiment is very good for carbon excitation, but for aluminum excitation the theory significantly overestimates the cross-section ratio. The influence of foil tilting and cascade contributions on the polarization were investigated experimentally and taken into account in the analysis of the measurements.

I. INTRODUCTION

The knowledge of the angular distribution and/or polarization of x radiation arising from the decay of atomic and ionic excited states produced in ion-atom collisions is important from several theoretical and practical viewpoints. The angular distribution and polarization of an x-ray line are determined by the relative magnetic substate population (or more generally by the alignment and orientation) of the excited states.[1,2] The magnetic substate cross sections provide more detailed information on the excitation mechanism than the total cross sections (summed over the magnetic substates), and hence measurement of the angular distribution enables detailed testing of the different collision theories and approximations. From a more practical point of view, the knowledge of the angular distribution and polarization is very important in interpreting absolute and relative intensity measurements, especially if the radiation is detected by polarization sensitive devices such as crystal spectrometers.

Despite considerable effort to clarify the mechanisms which govern the population of projectile states inside and at the surface of solids, a number of features are still puzzling.[3] In projectiles emerging from thin solid targets, high-lying Rydberg states are populated by excitation of projectile core electrons, capture of electrons from the solid, and possibly capture of convoy electrons at or near the foil surface. These Rydberg electrons cascade down to the lower states and give rise to a long-lived or "delayed" component of the x-ray intensities. The delayed components contribute to the measured intensities, and should be taken into account when the polarizations of the different x-ray lines are measured.

The target foil surface plays a very important role in beam-foil excitation of outer shells. Tilting the target surface with respect to the beam direction may influence the alignment of the projectile states, producing nonzero higher-order alignment tensor components and orientation of the excited states.[1] In the inner shell processes investigated here, the atomic character of the collision process is expected to dominate bulk or surface effects. However, the radiative lifetime of the $1s2p\ ^3P$ state is long enough to cause a significant contribution to the observed radiation from ions decaying behind the foil. Since radiative decay of the ^3P state occurs mainly for ions excited into this state at or near the back surface of the target foil, the question of the influence of the foil-surface inclination on the alignment of this state naturally arises, but has not been previously addressed.

Our previous investigation[4] of the $^1P_1$-$^1S_0$ and $^3P_1$-$^1S_0$ transitions of He-like sulfur excited by passage of 2-MeV/amu sulfur ions through a thin carbon foil revealed that these states are highly aligned. The relative substate population deduced from the measured angular distribution is in good agreement with the relative substate cross sections calculated by Reading and Ford[5] in their one-and-a-half-centered-expansion (OHCE) approximation[6,7] if it is assumed that the mechanism populating these states is electron capture from the K shell of carbon. This study demonstrated that measurement of the angular distribution is superior to polarization measurements using Brewster reflection[8] for the study of angular correlations

in ion-atom collisions, because it provides additional information on the otherwise unknown polarization sensitivity of the diffraction crystal itself.[9]

In the present investigation, angular distribution measurements were performed for the H- and He-like $2p$-$1s$ transitions of 2-MeV/amu Mg projectiles excited by passage through thin (50—70 $\mu g/cm^2$) carbon and aluminum foils. The primary purpose of this work was to test the theoretical calculations at significantly different projectile and target atomic numbers than had been done previously. Further motivation was provided by a recent study[10] of the spectra of H- and He-like Mg projectiles traveling in thin and thick solid carbon targets, which revealed that (i) the resolution of the ammonium dihydrogen phosphate (ADP) crystal for the Mg lines is superior to that of the NaCl crystal for S lines, (ii) relatively high-lying states ($n=4,5$) are populated to a measurable extent, (iii) the measured $^1P/^3P$ ratio significantly deviates from the expected value of one, indicating strong polarization.

To search for possible tilted foil effects on the alignment of the projectile states, the angular distributions of the $1s2p\ ^1P$ and $1s2p\ ^3P$ heliumlike lines of Mg projectiles excited by untilted and tilted ($\pm 45°$) carbon foils with same beam thicknesses have been measured and compared. To estimate the effect of the delayed component of the x-ray emission on the measured angular distributions, we have measured the ratio of the delayed x-ray intensity to the total intensity. The effect of this contribution on the measured polarization has been taken into account.

II. BACKGROUND OF THE METHOD

The measured angular distribution of an x-ray line is determined by the alignment and orientation of the excited state, the angular momentum of the initial and final state of the x-ray transition, and the properties of the detection system. In the mathematical formulation of angular correlation, the preceding factors are described by the orientation vector and alignment tensor of the excited state, and the angular momentum coefficients of the initial and final states and the emitted radiation, and the efficiency tensor of the detection apparatus. The general mathematical formulation of angular correlations can be found in standard textbooks and review articles.[1,2,11,12] The following discussion makes use of the Fano-Macek geometry convention and formulation[1,11,13] with some reference to the Percival-Seaton[2] formulation.

In cylindrically symmetric ion-atom collisions (where an unpolarized, unidirectional beam of ions excites or is excited by unpolarized target atoms), the cross section for production of the different magnetic substates of a given angular momentum state in the target or in the projectile depends on the absolute value of the magnetic quantum number but not upon the sign. Excited states produced in such collisions cannot be oriented, but they can be aligned if the angular momentum of the state is greater than $(\frac{1}{2})\hbar$. The angular distribution of electric-dipole radiation from aligned ions, measured by a crystal spectrometer with crystal planes oriented to accept radiation with the electric vector perpendicular to the quantization axis (beam direction) is given by

$$I(\theta)=(I_0/4\pi)R\epsilon\Omega[1-\tfrac{1}{2}\beta(1-3Q) + \tfrac{3}{2}\beta(1-Q)\cos^2\theta] , \quad (1)$$

where I_0 is the total intensity emitted into the 4π-rad solid angle, R is the reflectivity of the crystal for unpolarized radiation (usually referred to as reflectivity), ϵ is the efficiency of the detector used to count the x-ray photons reflected by the crystal (usually a flow-mode proportional counter), Ω is the solid angle of the spectrometer, Q is the polarization sensitivity of the crystal, β is the anisotropy parameter of the radiation, and θ is the detection angle. The anisotropy parameter β is related to the alignment tensor component $A_0^{\rm col}$ of Fano and Macek[1] by

$$\beta=-\tfrac{1}{2}h^{(2)}(j_i,j_f)A_0^{\rm col} ,$$

where $h^{(2)}(j_i,j_f)$ is the angular momentum coefficient which depends on the initial and final states of the x-ray transition. The relationship between the anisotropy parameter and the linear polarization fraction P measured at 90° to the beam direction is given by

$$P=3\beta/(\beta-2) . \quad (2)$$

The $A_0^{\rm col}$ alignment tensor component is simply related to the cross sections for producing the different magnetic substates of given excited states. By calculating the appropriate $h^{(2)}$ angular momentum coefficients, one obtains an equation which relates the anisotropy parameter (and hence the linear polarization) of a given x-ray line and magnetic substate cross sections. For the heliumlike $1s2p\ ^1P_1$–$1s2p\ ^1S_0$ and $1s2p\ ^3P_1$–$1s2p\ ^1S_0$ and the hydrogenlike $2p\ ^2P$–$2p\ ^2S$ (unresolved doublet) lines, the cross sections for production of the $|m|=0$ (σ_0) and $|m|=1$ (σ_1) magnetic substates of the $2p$ state are related to the linear polarization fraction at 90° by the following formulas:[2]

$$P(^1P)=(\sigma_0-\sigma_1)/(\sigma_0+\sigma_1) , \quad (3a)$$

$$P(^3P)=-(\sigma_0-\sigma_1)/(\sigma_0+3\sigma_1) , \quad (3b)$$

$$P(^2P)=3(\sigma_0-\sigma_1)/(7\sigma_0+11\sigma_1) . \quad (3c)$$

If the cylindrical symmetry of the collision is broken by having another distinguished direction (i.e., outgoing particles detected in coincidence with the radiation or an inclined foil surface), the higher-order components of the alignment tensor and the orientation vector can be different from zero. If this second distinguished direction is in the plane containing the beam direction and the spectrometer, the angular distribution of electric dipole radiation detected as described previously is given by

$$I(\theta)=(I_0/4\pi)R\epsilon\Omega[1-\tfrac{1}{2}\beta'(1-3Q)+\beta_2(1+3Q) + \tfrac{3}{2}\beta'(1-Q)\cos^2\theta - \tfrac{3}{2}\beta_1(1-Q)\sin(2\theta)] , \quad (4)$$

where the anisotropy parameters β', β_1, and β_2 are given by[1]

$$\beta' = -\tfrac{1}{2}h^{(2)}(A_0^{\mathrm{col}} - A_{2+}^{\mathrm{col}}) ,$$

$$\beta_1 = -\tfrac{1}{2}h^{(2)}A_{1+}^{\mathrm{col}} ,$$

$$\beta_2 = -\tfrac{1}{2}h^{(2)}A_{2+}^{col} .$$

If the radiation arises from excited target ions, the parameters R, ϵ, Ω and Q in Eq. (1) do not depend on the observation angle, and hence the anisotropy parameter β (and consequently the polarization fraction P) for a given x-ray line can be determined by fitting the measured angular distribution with Eq. (1) using β and I_0 as fitting parameters. The polarization sensitivity Q plays a crucial role and must be known to deduce the polarization from the fit.

If radiation from projectile states is observed, the measured angular distribution has to be fitted by Eq. (1) transformed into the laboratory frame of reference. This transformation is straightforward and the effect on the observation angle, on the solid angle, and on the observed x-ray energy (and consequently on ϵ) is easily taken into account. The effect of the Doppler shift on the reflectivity and polarization sensitivity is somewhat complicated by the fact that the dependence of these quantities on the x-ray energy is not known precisely. The reflectivity and the polarization sensitivity are not simply multiplicative factors (as in the case of target x rays), but depend on the observation angle due to the Doppler shift and thus affect the shape of the angular distribution. One can take advantage of this fact, however, by noting that information on these quantities may be deduced from the shape of the angular distribution itself. The measured angular distributions may be fitted with the transformed Eq. (1) by incorporating different theoretical reflectivity and polarization sensitivity functions into it. In addition to the determination of the polarization, this procedure leads to the determination of the most appropriate functional form of the reflectivity and polarization sensitivity of the crystal.

III. EXPERIMENTAL METHOD

A beam of 48-MeV Mg^{3+} ions from the variable energy cyclotron of Texas A&M University was directed onto thin targets which could be inclined at different angles to the beam direction around an axis perpendicular to the plane containing the beam and the spectrometer. The He- and H-like portions of the x-ray spectrum of the Mg projectiles were measured with a plane-crystal Bragg spectrometer rotatable around a pivot axis coincident with the target rotation axis. The beam intensity was monitored by measuring the intensity of the projectile x rays excited by a 20-$\mu g/cm^2$ carbon foil located upstream from the target using a proportional counter identical with that used in the crystal spectrometer. The other details of the experimental setup, the data acquisition system and the spectral analysis were the same as described earlier.[4,9]

When the angular distribution of the absolute intensity of an x-ray line is to be measured, the geometrical rotational symmetry of the measuring apparatus must be very precise. To check the rotational symmetry of the system, the angular distributions of the K x rays from a thin aluminum target excited by 5.5-MeV He^+ and 48-MeV Mg^{3+} beams were measured. The $K\alpha$ line, which dominates the He-excited spectrum, is unpolarized and isotropic. With Mg projectiles, the aluminum spectrum is dominated by the $K\alpha$ satellite lines, which may have slightly anisotropic angular distributions. The sum of the intensities of all the $K\alpha$ satellites, however, should be nearly isotropic. The measured angular distribution of the $K\alpha$ line excited by He bombardment and that of the total intensity of the $K\alpha$ satellites excited by Mg proved to be isotropic within the statistical error margins of $\pm 3\%$, which means that any geometric asymmetry of the system is below that error limit.

As pointed out in Sec. II, the knowledge of the dependence of the detection efficiency of the spectrometer on the x-ray energy is essential in the interpretation of the angular distribution of projectile x rays because this energy dependence introduces a detection angle dependence in the efficiency due to the Doppler shift. In the case of crystal spectrometers, the efficiency depends critically on the reflectivity of the diffracting crystal. Furthermore, the crystal spectrometer is inherently a polarization sensitive device since the reflectivity of the crystal (or more generally the detection efficiency of the crystal spectrometer) depends on the polarization of the detected x rays. In order to better understand the reflection properties of the ADP crystal used in this experiment, separate reflectivity measurements were performed as outlined in the following.

The reflection properties of a crystal may depend on its previous history and should be determined experimentally. The theory of crystal diffraction, however, provides useful guidelines. The reflection properties of a crystal can be characterized by the integrated reflectivity for unpolarized radiation, and by the polarization sensitivity.[9,14,15] Theoretically two extreme cases are distinguished: perfect crystal (with crystallites larger than 10^{-5} mm) and mosaic crystal (with crystallites smaller than 10^{-5} mm). The reflectivity and polarization sensitivity for these structures can be calculated theoretically.[14,15] The proper reflectivity function of a crystal, however, can be better described by taking absorption into account in the perfect and mosaic models.[9] These models will henceforth be referred to as the PCA (perfect crystal with absorption) and the MCA (mosaic crystal with absorption) models.

To determine the reflection properties of a crystal experimentally, one has to measure the reflectivity and the polarization sensitivity as functions of the x-ray energy. The polarization sensitivity measurements require a polarized x-ray source with known polarization, and it should be noted that synchrotron radiation presents interesting and useful possibilities in this regard. The determination of the reflectivity for unpolarized radiation is somewhat easier in the sense that it does not require a sophisticated x-ray source. As far as the relative intensity and angular distribution measurements[4] are concerned, only the relative reflectivity (i.e., the reflectivity normalized at a given x-ray energy) is required.

In the present work, the relative reflectivity of the ADP flat crystal was measured using an experimental setup which was basically the same as that used for the angular distribution measurements. Thick Mg, Al, Si, Li_2SO_4, P,

KCl, and CaO targets tilted at 45° with respect to the beam direction were bombarded with a beam of 5.5-MeV He ions. The K x-ray intensity was measured simultaneously with the crystal spectrometer and with a proportional counter identical to that used in the spectrometer mounted at 165° behind a small aperture. The spectrometer observation angle was 105°. The K x-ray intensity measured by the crystal spectrometer relative to that measured by the proportional counter depends on the relative solid angles of the two detectors and on the reflectivity of the crystal. Measuring this intensity ratio in a fixed geometry for different targets enables the determination of the relative reflectivities for the $K\alpha$ x rays of these elements. The $K\alpha$ satellites and the $K\beta$ lines are not resolved by the proportional counter, but using the satellite-to-$K\alpha$ and $K\beta$-to-$K\alpha$ ratios established by the crystal spectrometer measurements, a straightforward self-consistent correction can be made.

The reflectivity values measured relative to the reflectivity at 2.66 keV (Cl $K\alpha$) are shown in Fig. 1 together with the predictions of the PCA and MCA models. (The predictions of the perfect and mosaic models without absorption are in gross disagreement with the experimental results and are not shown in the figure.) The experimental data of McKenzie *et al.*[16] for a different ADP crystal are also shown for comparison. The experimental data are somewhere between the perfect and mosaic model, but give somewhat better agreement with the PCA model. These measurements are not very definitive with regard to the polarization sensitivity and a more direct determination of this important property is highly desirable. To emphasize the central importance of this quantity, the theoretical polarization sensitivity of the ADP crystal predicted by the perfect and mosaic models is shown in Fig. 2.

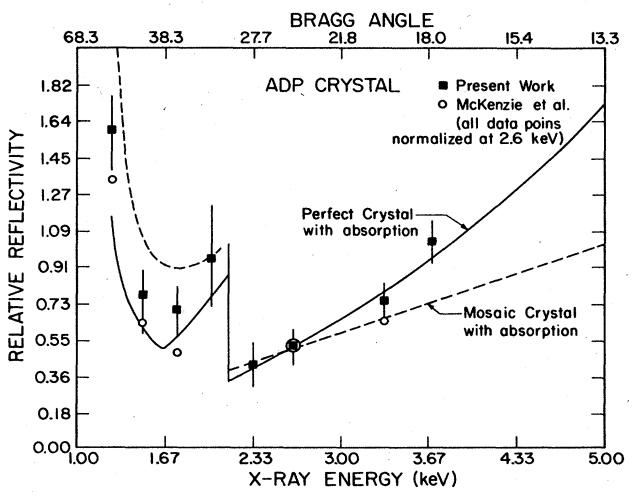

FIG. 1. Measured relative reflectivity of the ammonium dihydrogen phosphate (ADP) crystal. The solid curve is the prediction of the PCA model, and the broken curve is the prediction of the MCA model. The experimental data of McKenzie *et al.* (Ref. 16) are also shown.

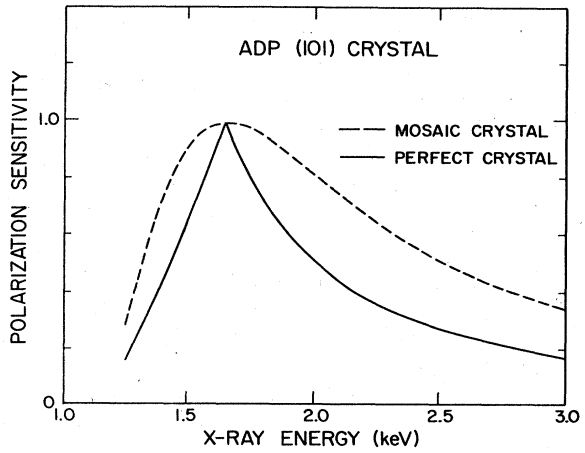

FIG. 2. Polarization sensitivity of the ammonium dihydrogen phosphate (ADP) crystal as a function of the x-ray energy according to the perfect (solid curve) and the mosaic (broken curve) models.

IV. RESULTS AND DISCUSSION

The spectra of the He- and H-like $2p$-$1s$ transitions of Mg projectiles obtained at observation angles of 90° and 161° shown in Fig. 3 clearly show the change in the

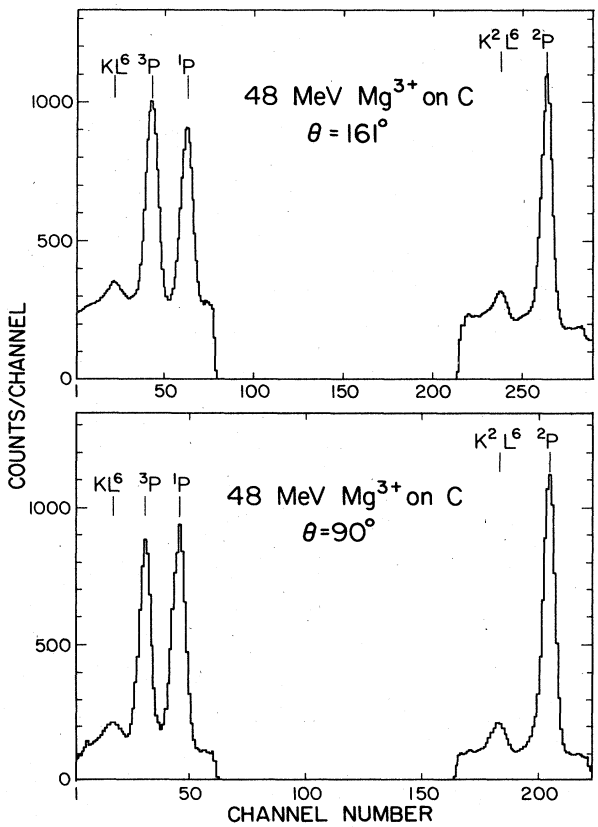

FIG. 3. Spectra of the He- and H-like $2p$-$1s$ transitions of 2-MeV/amu Mg projectiles excited by passing through a 50-$\mu g/cm^2$ carbon foil tilted at ±45° to the beam direction, obtained at observation angles 90° and 161°.

$I(^3P)/I(^1P)$ intensity ratio with observation angle. Spectra taken at the various observation angles were analyzed in the same manner by means of a least-squares fitting program (FACELIFT) using linear functions for the flat background and Voigt functions for the x-ray lines. The ^1P, ^3P, and ^2P lines are emitted partly inside and partly outside of the target foil. The measured intensities were corrected for absorption in the target foil using a simple model developed by Watson *et al.*[17] to estimate the fraction of the intensity emitted outside the foil. The polarizations of the ^1P, ^2P, and ^3P lines were determined by fitting their measured angular distributions with Eq. (1) using I_0 and the anisotropy parameter β as fitting parameters. The anisotropy parameters were converted into linear polarizations according to Eq. (2).

As was pointed out in Sec. III, the crystal reflectivity measurements led to the conclusion that the reflection properties were closer to the PCA than to the MCA model, but this conclusion was not totally unambiguous with regard to the polarization sensitivity. To obtain further understanding of this important quantity, an attempt was made to deduce information on the polarization sensitivity from the measured angular distribution itself. Two separate fits were made to each angular distribution, applying the PCA and the MCA models for the reflectivity and polarization sensitivity in Eq. (1). In Fig. 4 the fits to the angular distribution of the ^3P, ^1P, and ^2P lines, obtained using the PCA and MCA models, are compared. The PCA model obviously gives better fits to the experimental data than the MCA model for the ^3P and ^1P lines. The fit to the angular distribution of the ^2P line is not so selective, since the shape of the angular distribution is relatively insensitive to the crystal structure in this x-ray energy region.

As can be seen from Eq. (3) the polarizations of the ^3P and ^1P lines are determined by the σ_0/σ_1 cross-section ratio, where σ_0 and σ_1 are the respective cross sections for production of the $1s2p(|m|=0)$ and $1s2p(|m|=1)$ heliumlike states of the projectile. These are essentially the cross sections for capturing an electron from the target into the $2p$ state by a hydrogenlike projectile having a $1s$ electron. The polarizations deduced from the fits to the angular distributions of the ^1P and ^3P lines should, therefore, correspond to the same σ_0/σ_1 cross-section ratio. The cross-section ratios derived from the ^3P and ^1P polarizations using the PCA model are in excellent agreement $[(\sigma_0/\sigma_1)_{^3P}=1.74, (\sigma_0/\sigma_1)_{^1P}=1.74]$, whereas those extracted by using the MCA model disagree, $[(\sigma_0/\sigma_1)_{^3P}=4.41, (\sigma_0/\sigma_1)_{^1P}=2.03]$.

The σ_0/σ_1 cross-section ratio calculated from the ^2P polarization may in principle be different from that calculated from the ^3P and ^1P polarizations because in the case of the ^2P line σ_0 and σ_1 are the respective cross sections for production of the $2p(|m|=0)$ and $2p(|m|=1)$ hydrogenlike states of the projectile (i.e., they are essentially the cross sections for capturing an electron from the target into the $2p$ state by a bare projectile). In practice, however, the cross sections (and the cross-section ratios) for the preceding two processes cannot differ dramatically, because the presence of the $1s$ electron will not strongly alter the cross section for capture into the $2p$ states. Comparison of the σ_0/σ_1 ratios obtained from the ^2P polarization $[(\sigma_0/\sigma_1)_{MCA}=5.4, (\sigma_0/\sigma_1)_{PCA}=2.0]$ with the same ratios obtained from the ^1P and ^3P polarizations shows that use of the PCA model results in reasonable

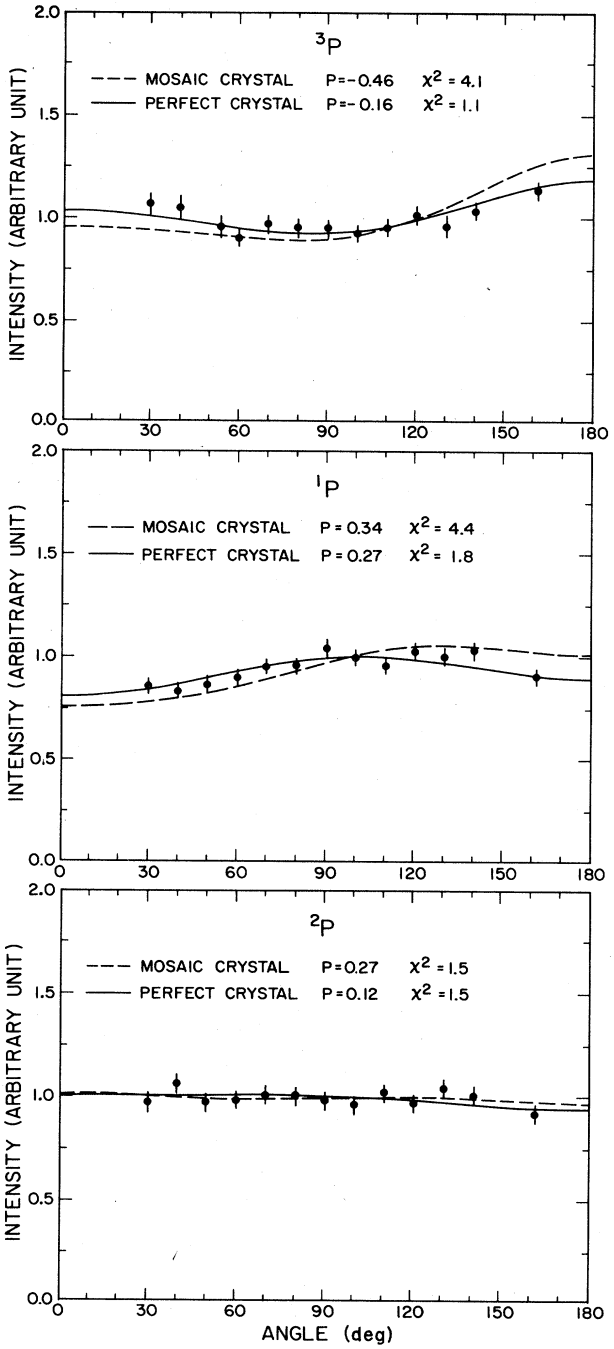

FIG. 4. Measured angular distributions of the ^1P, ^3P, and ^2P lines of 2-MeV/amu Mg projectiles excited by passing through a 50-μg/cm^2 carbon foil tilted at $\pm 45°$ to the beam direction. The solid curve is the fit of Eq. (1) to the experimental data using the PCA model, and the broken curve is the fit obtained using the MCA model. The deduced polarizations and the relative chi-squares are displayed in the figure.

values (i.e., the cross-section ratios are nearly the same), while the MCA model gives unreasonably different values.

There is yet another way to deduce the polarizations of the preceding lines and thereby check the consistency of the data analysis. The angular distributions of the intensity ratios can be measured more precisely than those of the absolute intensities. In the case of the $I(^3P)/I(^1P)$ ratio, a further advantage is that one can use the relationship between the ^3P and ^1P polarizations [see Eq. (3)], and thus use only one polarization as a fitting parameter. In the case of the $^2P/^1P$ ratio one can use the polarization of the ^1P line deduced from the fits to the angular distribution of the ^1P intensity, or that of the $^3P/^1P$ intensity ratio, and use only the ^2P polarization as a fitting parameter. In Fig. 5 the fits to the angular distributions of the $^3P/^1P$ and $^2P/^1P$ intensity ratios, assuming PCA and MCA models, are shown. The PCA model again gives good fits and the deduced polarization values are in agreement with those deduced from the fits to the angular distributions of the absolute intensities. The MCA model gives worse fits than the PCA model, and the deduced polarization of the ^2P line is unreasonable because the maximum possible value of the ^2P polarization is 0.43 ($\sigma_1=0$). Thus, the conclusion of these analyses is that the reflection and polarization properties of the ADP crystal used in this experiment are well described by the PCA model. The same conclusion was reached for the NaCl crystal used in the previous measurements of sulfur projectile x rays.[4,9]

When highly charged projectiles pass through a thin foil, electrons are frequently captured into high-lying Rydberg states of the projectiles at the surface of the foil and subsequently cascade down to the inner shells. The end of the cascading process is an x-ray transition which is delayed compared to the prompt decay of the same states produced by direct excitation or ionization. The mechanism populating these states has been extensively studied, and the decay curves measured, but several puzzling questions remain unanswered.[3,18] From the point of view of the present angular distribution study, the cascade contribution may influence the measurements in two ways: (i) the delayed component decays well behind the foil and hence the spectrometer may see different portions of the delayed intensity at different observation angles, (ii) it is reasonable to assume that the delayed radiation is isotropic and unpolarized since it is the result of a long cas-

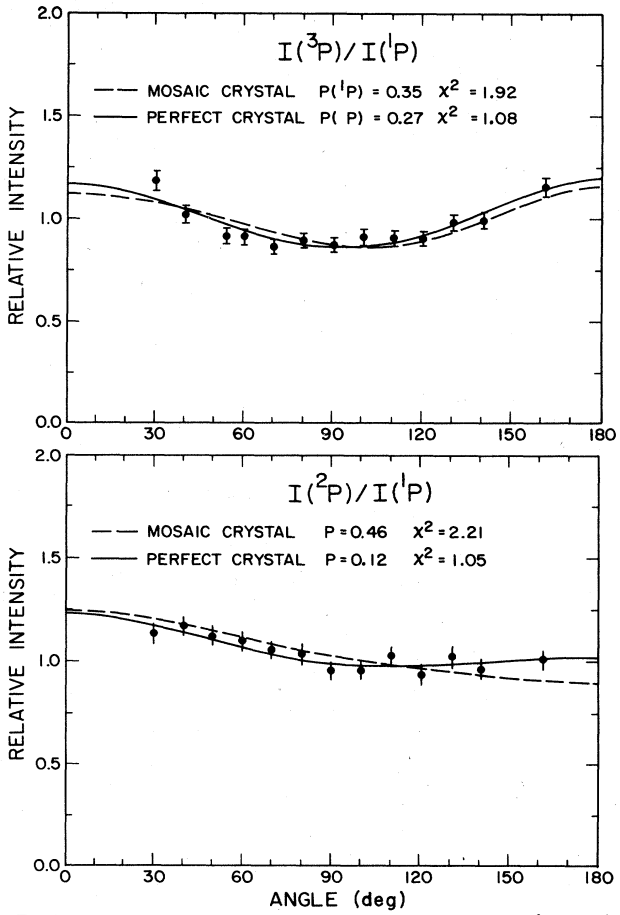

FIG. 5. Measured angular distributions of the $I(^3P)/I(^1P)$ and $I(^2P)/I(^1P)$ intensity ratios for 2-MeV/amu Mg projectiles excited by passing through a 50-μg/cm^2 carbon foil tilted at $\pm45°$ to the beam direction. The solid curve is the fit of Eq. (1) to the experimental data using the PCA model, and the broken curve is the fit obtained using the MCA model. The deduced polarizations and the relative chi-squares are displayed in the figure.

TABLE I. The measured polarizations of the ^3P, ^1P, and ^2P lines of He- and H-like 2-MeV/amu Mg projectiles excited by thin carbon foils measured under different experimental conditions. The corresponding σ_0/σ_1 cross-section ratios are also given.

X-ray line	Polarization	σ_0/σ_1
	Excitation by 50-μg/cm^2 carbon foil tilted at $\pm45°$	
^3P	-0.16 ± 0.06	1.76 ± 0.30
^1P	0.28 ± 0.05	1.78 ± 0.20
^2P	0.13 ± 0.06	2.13 ± 0.60
$^1P(^3P/^1P)$	0.29 ± 0.04	1.82 ± 0.16
$^2P(^2P/^1P)$	0.13 ± 0.05	2.13 ± 0.50
	Excitation by 70-μg/cm^2 untilted carbon foil	
^3P	-0.21 ± 0.06	2.06 ± 0.36
^1P	0.31 ± 0.06	1.90 ± 0.24
$^1P(^3P/^1P)$	0.33 ± 0.05	1.98 ± 0.20

cade process involving many transitions.

In order to estimate the importance of the cascade component, the contribution of the delayed x rays to the total emitted intensity was measured. With the spectrometer positioned at 90° and the target foil oriented perpendicular to the beam direction (the normal vector of the foil surface parallel to the beam), the spectrometer cannot see the radiation emitted inside or at the surface of the foil, but will only detect the radiation emitted behind the foil. By masking out different portions of the Soller collimator in this arrangement, the intensities of the delayed components for the ^3P, ^1P, and ^2P lines were measured as a function of the observation distance behind the foil. The results of this measurement showed that the intensity of the delayed radiation emitted behind the foil at distances greater than 4 mm ($\sim$0.2 ns flight time) contribute less than 1% to the total intensity, but the total contributions of the delayed x rays to the measured intensities are $\sim$6—8 %. This means that the spectrometer sees the whole radiating volume at each observation angle, but the polarizations deduced from the measured angular distributions have to be corrected for the isotropic delayed contribution. If an unpolarized component is detected together with a polarized one, the polarization deduced from the angular distribution has to be corrected to get the polarization of the anisotropic component. Simple mathematical manipulation shows that the corrected polarization P_c is given by

$$P_c=\frac{1+k}{1+\frac{1}{3}kP}P\ ,$$

where P is the polarization deduced from the fit, and k is the ratio of the intensity of the anisotropic component to the total intensity. This correction amounts to a 5—7 % correction to the polarization of the different lines, and the experimental results given in Tables I and III are the corrected values.

As was briefly summarized earlier in Sec. II, the surface of the target foil may in principle influence the alignment of the projectile states, resulting in a dependence of the polarization of the emitted radiation on the tilt angle of the foil surface. The measurements discussed so far were carried out with 50-μg/cm^2 carbon foils tilted at $\pm$45° with respect to the beam direction. The fact that these angular distributions can be fitted well with Eq. (1) indicates that foil tilting has no strong effect on the shape of the angular distribution. To check the effect of tilting the foil more directly, a set of measurements were carried out with a 70 μg/cm^2 untilted carbon foil. The measured angular distribution of the $I(^3P)/I(^1P)$ intensity ratio is shown in Fig. 6. The fit to the data points was made using the PCA model in Eq. (1).

The polarizations of the different lines (corrected for delayed x rays) deduced from the angular distribution measurements are summarized in Table I. The polarizations deduced from the untilted foil measurements are somewhat larger than those obtained with the tilted ones, but this difference is not beyond the error margins of the measurements.

Several mechanisms may contribute to the production of the He- and H-like $2P$ states of Mg projectiles passing through thin carbon foils. The capture of electrons into the $2p$ state of H-like and bare projectiles from the target is the most probable process producing these states. In Table II we compare the σ_0/σ_1 cross-section ratios corresponding to the measured polarizations with the theoretical σ_0/σ_1 cross-section ratio calculated in different approximations for the capture of electrons from the K shell of carbon into the $2p(|m|=0)$ and $2p(|m|=1)$ magnetic substates of the Mg projectiles. The theoretical approximations which are compared to the experimental data are the Oppenheimer-Brinkman-Kramers approximation (OBK), the first Born approximation (BA), the single-centered-expansion calculation (SCE), and the perturbative one-and-a-half-centered-expansion calculation (OHCE) of Reading *et al.*[5–7] The OBK approximation, which is frequently used for estimation of capture cross sections, is in gross disagreement with the present experimental data. The BA calculation gives results closer to the experimental data, but significantly overestimates the σ_0/σ_1 cross-section ratio beyond the error margins of the experimental data. The OHCE calculation gives excellent agreement with the present experimental data. The OHCE also gave good agreement with the experimental data on the polarization of the He-like lines of sulfur excited by thin carbon foils,[4] but in that case the difference between the OBK and the OHCE approximations was not as dramatic as for the Mg on the carbon system.

The experimental σ_0/σ_1 cross-section ratio increases as the atomic number of the projectile decreases from S ($Z=16$) to Mg ($Z=12$). The OHCE approximation reproduces this dependence very well, while the OBK approximation gives a much steeper dependence. The

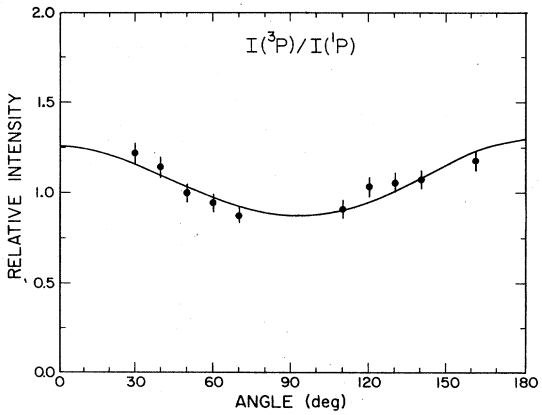

FIG. 6. Measured angular distribution of the $I(^3P)/I(^1P)$ intensity ratio for 2-MeV/amu Mg projectiles excited by passing through a 70-μg/cm^2 untilted carbon foil. The solid curve is the fit of Eq. (1) to the experimental data using the PCA model.

TABLE II. The present experimental σ_0/σ_1 cross-section ratio for carbon foil-excited Mg projectiles is compared with the results of the theoretical calculations discussed in the text.

	Theoretical calculations				
	OHCE	SCE	OBK	BA	Experiment
σ_0/σ_1	1.93	1.93	4.59	2.84	1.95±0.20

OHCE approximation predicts a more complicated dependence on the projectile atomic number. The calculated ratio increases as the projectile atomic number decreases from $Z=18$ (Ar) to $Z=13$ (Al), where it has a maximum. It then decreases as the atomic number decreases. This dependence is not yet fully confirmed by experiments and it is desirable to extend the measurements (e.g., to Ne projectiles) to check this predicted atomic number dependence.

Besides the projectile Z dependence, another interesting question concerns how the polarizations of the H- and He-like lines of the projectile depend on the target material. In the course of checking the rotational symmetry of our apparatus, measurements were carried out on the angular distribution of target x rays from thin aluminum targets using 5.5-MeV He and 2-MeV/amu Mg ions. In the measurements with Mg ions, the He-like lines of the Mg projectiles could be measured at all observation angles without interference from the Al target x rays. The angular distribution of the $^3P/^1P$ intensity ratio obtained with a 50-μg/cm^2 Al target is shown in Fig. 7. The solid curve is the fit of Eq. (1) to the measured data using the PCA model. In Table III the σ_0/σ_1 cross-section ratios corresponding to the polarizations deduced from the fits to the angular distributions are summarized, and in Table IV they are compared with the results of the theoretical calculations discussed before.

The experimental polarizations obtained with the two foil materials are not significantly different. The theoretical calculations, however, give very different σ_0/σ_1 ratios for Al and C excitation, and the experimental σ_0/σ_1 ratio for Al excitation is in gross disagreement with the theoretical results. The OBK and the BA calculations even give opposite signs for the polarization, while the OHCE and the SCE give the sign of the polarization in agreement with the experiment, but give much higher σ_0/σ_1 ratios.

It must be noted, that for Al, the comparison of the experimental and theoretical data is complicated by the presence of an aluminum-oxide layer on the target. The thin Al targets were prepared by vacuum evaporation and stored in dry atmosphere, but it is known that a $\sim$30-Å Al_2O_3 layer builds up on the surface very quickly.[19] This aluminum-oxide layer corresponds to $\sim$0.5 μg/cm^2 effective oxygen thickness, which gives a small contribution to the capture. Another experimental factor complicating the comparison is the possible deposition of carbon on the targets. The scattering chamber was pumped by a turbomolecular pump to $\sim 10^{-5}$ Torr vacuum, and while the reproducibility of the intensity measurements did not indicate serious target thickening, they are not sensitive enough to detect carbon deposition less than a few μg/cm^2. Therefore the possibility that carbon layers on the exit surface of the Al target influenced the experimental data, cannot be ruled out entirely. The surface conditions would effect the ^3P line more than the ^1P, because the fraction of the intensity emitted inside the foil is significantly higher for the ^1P line.[17] The σ_0/σ_1 ratios deduced from the ^1P and ^3P intensities, however, are very close and therefore do not indicate strong surface effects. Further investigation of this particular problem, however, would be desirable.

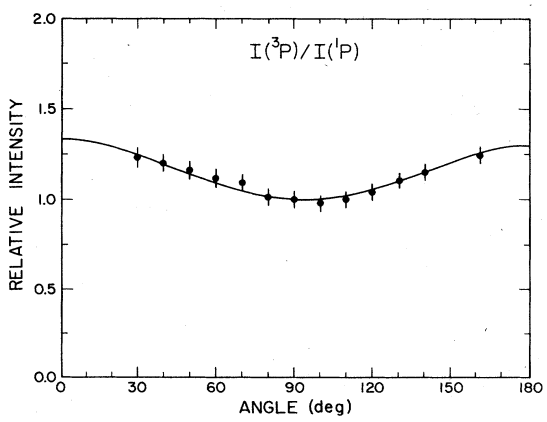

FIG. 7. Measured angular distribution of the $I(^3P)/I(^1P)$ intensity ratio for 2-MeV/amu Mg projectiles excited by passing through a 50-μg/cm^2 aluminum foil tilted at $\pm 45°$ to the beam direction. The solid curve is the fit of Eq. (1) to the experimental data using the PCA model.

TABLE III. The measured polarizations of the He-like ^3P and ^1P lines of 2-MeV/amu Mg projectiles excited by thin (50 μg/cm^2) aluminum foil tilted at $\pm 45°$. The corresponding σ_0/σ_1 cross-section ratios are also given.

X-ray line	Polarization	σ_0/σ_1
^3P	-0.15 ± 0.05	1.71 ± 0.18
^1P	0.32 ± 0.06	1.94 ± 0.20
$^1P(^3P/^1P)$	0.26 ± 0.05	1.70 ± 0.16

More likely reasons for the large discrepancy between the experimental and theoretical results for Al are the following: (i) the theoretical calculations do not provide satisfactory descriptions for symmetric collisions; (ii) the capture into the $2p$ states of the Mg projectiles proceeds primarily from levels above the K shell of Al. In the preceding theoretical calculations, only capture from the K shell of the target is included. The breakdown of the OBK and BA calculations is not surprising, and the fact that the OHCE approximation gives the observed sign of the polarization indicates that this calculation might provide a good description of the $1s$-$2p$ capture even for the nearly symmetric Mg-Al system. Unfortunately, the measurement of the polarizations of the He-like lines of the projectile produced in pure $1s$-$2p$ capture requires coincidence measurements. The theoretical calculation of the $2s$-$2p$ and $2p$-$2p$ capture for the Mg-Al system, however, would be highly desirable for comparison with the present results.

TABLE IV. The present experimental σ_0/σ_1 cross-section ratio for aluminum foil-excited Mg projectiles is compared with the results of the theoretical calculations discussed in the text.

	Theoretical calculations				
	OHCE	SCE	OBK	BA	Experiment
σ_0/σ_1	7.80	7.87	0.68	0.96	1.78 ± 0.20

ACKNOWLEDGMENTS

We wish to acknowledge helpful discussions with Professor A. L. Ford and Professor J. F. Reading and the use of their unpublished calculations. This research was supported by the Division of Chemical Sciences of the U.S. Department of Energy, the Robert A. Welch Foundation, the Texas A&M University Center for Energy and Mineral Resources, and the National Science Foundation.

---

*On leave from Institute of Nuclear Research of the Hungarian Academy of Sciences, Debrecen, Hungary.

†Present address: Peking Normal University, Peking, China.

[1]U. Fano and J. Macek, Rev. Mod. Phys. **45**, 553 (1973).

[2]I. C. Percival and M. J. Seaton, Philos. Trans. R. Soc. (London) **A251**, 113 (1958).

[3]H.-D. Betz, D. Roschenthaler, and J. Rothermel, Phys. Rev. Lett. **50**, 34 (1983).

[4]D. A. Church, R. A. Kenefick, D.-W. Wang, and R. L. Watson, Phys. Rev. A **26**, 3093 (1982).

[5]J. F. Reading and A. L. Ford (private communications).

[6]J. F. Reading, A. L. Ford, and R. L. Becker, J. Phys. B **14**, 1995 (1981).

[7]J. F. Reading, A. L. Ford, and R. L. Becker, J. Phys. B **15**, 625 (1982).

[8]L. D. Ellsworth, B. L. Doyle, U. Schiebel, and James R. MacDonald, Phys. Rev. A **19**, 943 (1979).

[9]D.-W. Wang, R. L. Watson, R. A. Kenefick, and D. A. Church, Nucl. Instrum. Methods **202**, 355 (1982).

[10]R. J. Maurer, R. L. Watson, and G. J. Pedrazzini, Nucl. Instrum. Methods **214**, 117 (1983).

[11]U. Fano and G. Racah, *Irreducible Tensorial Sets* (Academic, New York, 1959).

[12]S. Devon and L. J. B. Goldfarb, in *Handbuch der Physik,* edited by S. Flugge (Springer, Berlin, 1957), Vol. 42, p. 362.

[13]L. A. Morgan and M. R. C. McDowell, Comments At. Mol. Phys. **7**, 123 (1978).

[14]B. E. Warren, *X-ray Diffraction* (Addison-Wesley, Reading, Mass., 1969).

[15]B. Cleff, Acta Phys. Pol. A **61**, 285 (1982).

[16]D. L. McKenzie, P. B. Landecker, and J. H. Underwood, Space Sci. Instrum. **2**, 125 (1976).

[17]R. L. Watson, A. Langenberg, R. A. Kenefick, C. C. Bahr, and J. R. White, Phys. Rev. A **23**, 2471 (1981).

[18]E. P. Kanter, D. Schneider, and Z. Vager, Phys. Rev. A **28**, 1193 (1983).

[19]R. K. Hart, Proc. R. Soc. (London) Ser. A **236**, 68 (1956).